Revision 1

Ferriphoxite and carboferriphoxite: two new oxalato-phosphate minerals from the Rowley mine, Arizona, USA

Anthony R. Kampf[1*], Chi Ma[2], Frank C. Hawthorne[3] and Joe Marty[1]

[1] Mineral Sciences Department, Natural History Museum of Los Angeles County, 900 Exposition Boulevard, Los Angeles, California 90007, USA

[2] Division of Geological and Planetary Sciences, California Institute of Technology, 1200 East California Boulevard, Pasadena, California 91125, USA

[3] Department of Geological Sciences, University of Manitoba, Winnipeg, Manitoba, R3T 2N2, Canada

*E-mail: akampf@nhm.org

Abstract

Ferriphoxite, $[(NH_4)_2K(H_2O)][Fe^{3+}(HPO_4)_2(C_2O_4)]$, and carboferriphoxite, $[(NH_4)K(H_2CO_3)][Fe^{3+}(HPO_4)(H_2PO_4)(C_2O_4)]$, are new mineral species from the Rowley mine, Maricopa County, Arizona, U.S.A. They occur with antipinite, aphthitalite, baryte, fluorite, hematite and quartz in an unusual bat-guano-related, post-mining assemblage. Ferriphoxite occurs as rectangular blades, up to about 0.1 mm in length, typically forming

DOI: 10.1180/mgm.2024.56

https://doi.org/10.1180/mgm.2024.56 Published online by Cambridge University Press

sprays. Carboferriphoxite occurs as needles or blades, up to about 0.2 mm in length, typically forming fan- and bowtie-like sprays. Both species are colourless with white streak, vitreous lustre, ~2 Mohs hardness, brittle tenacity and splintery fracture. Ferriphoxite has three good cleavages ({100}, {010} and {001}) and carboferriphoxite has two good cleavages (probably {100} and {001}). Both species have a measured density of 2.14(2) $g\cdot cm^{-3}$. Ferriphoxite is biaxial (+) with α = 1.524(3), β = 1.560(3), γ = 1.608(3) and $2V_{meas.}$ = 83.9(4)°. Carboferriphoxite is biaxial (+) with α = 1.525(3), β = 1.555(calc), γ = 1.630(3) and $2V_{meas.}$ = 67(1)°. Electronprobe microanalysis gave $\{[(NH_4)_{2.13}K_{0.87}]_{\Sigma 3.00}(H_2O)\}\{(Fe^{3+}_{0.95}Al_{0.05})_{\Sigma 1.00}(HPO_4)_2(C_2O_4)\}$ for ferriphoxite and $\{[(NH_4)_{1.12}K_{0.88}]_{\Sigma 2.00}(H_2CO_3)\}\{(Fe^{3+}_{0.78}Al_{0.22})_{\Sigma 1.00}(HPO_4)(H_2PO_4)(C_2O_4)\}$ for carboferriphoxite. Ferriphoxite is monoclinic, $P2_1/c$, with a = 11.389(5), b = 6.352(3), c = 18.716(9), β = 102.887(9)°, V = 1319.8(11) Å^3 and Z = 4. Carboferriphoxite is triclinic, P-1, with a = 6.4405(3), b = 9.399(5), c = 11.839(6) Å, α = 95.763(10), β = 92.314(10), γ = 100.665(8)°, V = 695.6(6) Å^3 and Z = 2. The structures of ferriphoxite (R_1 = 0.0678 for 1850 $I > 2\sigma_I$ reflections) and carboferriphoxite (R_1 = 0.0427 for 3602 $I > 2\sigma_I$ reflections) both contain double-strand chains of corner-sharing $Fe^{3+}O_6$ octahedra and $PO_3(OH)$ tetrahedra. The chain in ferriphoxite is decorated by PO_3OH tetrahedra and C_2O_4 groups and that in carboferriphoxite is decorated by $PO_2(OH)_2$ tetrahedra and C_2O_4 groups. The interstitial units in both structures contain K^+ and NH_4^+ cations along with a H_2O group in ferriphoxite and H_2CO_3 group in carboferriphoxite.

Keywords: ferriphoxite; carboferriphoxite; new mineral species; oxalate; phosphate; crystal structure; Rowley mine, Arizona.

Introduction

Ferriphoxite and carboferriphoxite are closely related new mineral species found in an unusual bat guano assemblage in the Rowley mine in southwestern Arizona (USA). The name ferriphoxite is based on the composition of the structural unit – a linkage of ferric-iron octahedra, hydrogen phosphate tetrahedra and oxalate groups. The same structural unit is found in the associated mineral carboferriphoxite, which contains a dihydrogen carbonate (carbonic acid) group in its interstitial complex. Both minerals also contain NH_4 and K sites in their interstitial complexes. We do not see a need at this point to add suffixes to either name; however, if analogues with different dominances at the large-cation sites were to be found, K and NH_4 suffixes could be added based on the overall dominance of NH_4 or K summed over all the large cation sites, in which case ferriphoxite would become ferriphoxite-(NH_4) and carboferriphoxite would become carboferriphoxite-(NH_4).

The new minerals and their names were approved by the Commission on New Minerals, Nomenclature and Classification of the International Mineralogical Association. Type specimens are deposited in the collections of the Natural History Museum of Los Angeles County, Los Angeles, California, USA. Catalogue number 76303 is the holotype for ferriphoxite (IMA 2023-096; Warr symbol: Fphx) and the cotype for carboferriphoxite (IMA 2023-097; Warr symbol: Cfphx). Catalogue number 76304 is the holotype for carboferriphoxite and the cotype for ferriphoxite.

Occurrence

Ferriphoxite and carboferriphoxite were collected by one of the authors (JM) on February 1, 2016, on the 125-foot level of the Rowley mine, about 30 km NNW of Gila Bend (the nearest town to the mine), Maricopa County, Arizona, USA (33°2'57"N 113°1'49.59"W). The Rowley mine is on the western slope of the Painted Rock Mountains (in the Painted Rock mining district) and overlooks the Dendora Valley, immediately to the west. It is a former Cu-Pb-Au-Ag-Mo-V-baryte-fluorspar mine that exploited veins presumed to be related to the intrusion of an andesite porphyry dike into Tertiary volcanic rocks. Although

https://doi.org/10.1180/mgm.2024.56 Published online by Cambridge University Press

the mine has not been operated for ore since 1923, collectors took notice of the mine as a source of fine wulfenite crystals around 1945. An up-to-date account of the history, geology and mineralogy of the mine was recently published by Wilson (2020).

The new minerals were found in a hot and humid area of the mine (see Fig. 26 in Wilson, 2020) in an unusual bat guano-related, post-mining assemblage of phases that include a variety of vanadates, phosphates, oxalates and chlorides, some containing $(NH_4)^+$. This secondary mineral assemblage is found growing on baryte-quartz-rich matrix and, besides ferriphoxite and carboferriphoxite, includes allantoin (2020-004; Kampf *et al.*, 2021a), alunite, ammineite, antipinite, aphthitalite, bassanite, biphosphammite, cerussite, davidbrownite-(NH_4) (2018-129; Kampf *et al.*, 2019a), dendoraite-(NH_4) (2020-103; Kampf *et al.*, 2022a), ebnerite (2022-123), edwindavisite (2023-056), epiebnerite (2023-066), fluorite, halite, hydroglauberite, mimetite, mottramite, natrosulfatourea (2019-134; Kampf *et al.*, 2021a), newberyite, perite, phoxite (2018-009; Kampf *et al.*, 2019b), relianceite-(K) (2020-102; Kampf *et al.*, 2022a), rowleyite (2016-037; Kampf *et al.*, 2017), salammoniac, struvite, thebaite (2020-072; Kampf *et al.*, 2021b), thenardite, urea, vanadinite, weddellite, willemite, wulfenite and several other potentially new minerals. Ferriphoxite and carboferriphoxite were found in intimate association with antipinite, aphthitalite, baryte, fluorite, hematite and quartz. The new minerals are the result of the interaction of bat excrement with the existing mineralization in the mine.

Physical and Optical Properties

Ferriphoxite

Crystals of ferriphoxite are colourless rectangular blades, up to about 0.1 mm in length, typically occurring in sprays (Fig. 1). The blades are flattened on {001}, elongated along [010] and exhibit the forms {100}, {010} and {001}. No twinning was observed.

https://doi.org/10.1180/mgm.2024.56 Published online by Cambridge University Press

Ferriphoxite has a white streak, vitreous luster, brittle tenacity and splintery fracture. The Mohs hardness is about 2 based on scratch tests. There are two good cleavages in the [010] zone – probably {100} and {001}. The mineral does not fluoresce in either long- or short-wave ultraviolet illumination. The density measured by flotation in a mixture of methylene-iodide and toluene is 2.14(2) g·cm^{-3}. The calculated density is 2.138 g·cm^{-3} using the empirical formula and single-crystal unit-cell volume. At room-temperature, ferriphoxite is insoluble in H_2O, but easily soluble in dilute HCl. Ferriphoxite is optically biaxial (+) with α = 1.524(3), β = 1.560(3), γ = 1.608(3) (determined in white light). The measured $2V$ using extinction data analysed with EXCALIBR (Gunter *et al*., 2004) is 83.9(4)°; the calculated $2V$ is 84.1°. There is distinct $r < v$ dispersion. The optical orientation is $X = \mathbf{b}$, $Y \approx \mathbf{c}$, $Z \approx \mathbf{a^*}$ and the mineral is nonpleochroic.

Carboferriphoxite

Carboferriphoxite occurs as colourless needles or blades, up to about 0.2 mm in length, typically forming fan- and bowtie-like sprays (Fig. 2). Crystals are flattened on {010}, elongated along [100], have flat terminations and exhibit the forms {100}, {010} and {001}. No twinning was observed. Carboferriphoxite has a white streak, vitreous luster, brittle tenacity and splintery fracture. The Mohs hardness is about 2 based on scratch tests. There are three good cleavages: {100}, {010} and {001}. The mineral does not fluoresce in either long- or short-wave ultraviolet illumination. The density measured by flotation in a mixture of methylene-iodide and toluene is 2.14(2) g·cm^{-3}. The calculated density is 2.122 g·cm^{-3} using the empirical formula and single-crystal XRD unit-cell volume. At room-temperature, the mineral is insoluble in H_2O, but easily soluble in dilute HCl. Carboferriphoxite is optically biaxial (+) with α = 1.525(3), β = 1.555(calc), γ = 1.630(3) (determined in white light). The measured $2V$ using extinction data analysed with EXCALIBR (Gunter *et al*., 2004) is 67(1)°. It proved difficult to measure β, so it has been calculated from α, γ and $2V$. It

https://doi.org/10.1180/mgm.2024.56 Published online by Cambridge University Press

was not possible to observe the interference figure, so dispersion could not be determined. The optical orientation is $X \approx$ **a**, $Y \approx$ **b***, $Z \approx$ **c** and the mineral is nonpleochroic. Note that a good way to distinguish carboferriphoxite from ferriphoxite is by its distinctly higher birefringence, evidenced by higher order interference colours under crossed polars.

Raman spectroscopy

Raman spectroscopy for ferriphoxite and carboferriphoxite was done on a Horiba XploRA PLUS spectrometer. Both minerals are very sensitive to both the 532 and 785 nm lasers. We were able to obtain spectra from 3800 to 60 cm^{-1} using a 532 nm diode laser at 10% power (2 mW) using a 200 μm slit, an 1800 gr/mm diffraction grating and a 100× (0.9 NA) objective; however, the spectra exhibit significant noise. This, coupled with the complexities of the spectra, made definite interpretations for all bands difficult. The spectra are shown in Figure 3 and are labelled with tentative mode assignments based on several references including Frost *et al.* (2008a,b), Frost *et al.* (2011), Sergeeva *et al.* (2019), Števko *et al.* (2018) and Yakovenchuk *et al.* (2018).

Most of the features in the spectra result from phosphate and oxalate groups in the topologically equivalent chains in the structures; hence, the spectra are very similar. A difference of note is the very sharp band at 1384 cm^{-1} in the carboferriphoxite spectrum, which is not present in the ferriphoxite spectrum. This band is assignable to the $\nu_3(CO_3)$ antisymmetric stretching mode of the dihydrogen carbonate group, which is a component of the interstitial complex only in the carboferriphoxite structure.

Chemical Analysis

Analyses (4 points for ferriphoxite and 6 points for carboferriphoxite) were done at Caltech on a JEOL JXA-iHP200F field-emission electron microprobe (EPMA) in WDS

https://doi.org/10.1180/mgm.2024.56 Published online by Cambridge University Press

mode. Analytical conditions were 15 kV accelerating voltage, 10 nA beam current and a focused beam. Because of the small size, thinness and fragility of the crystals, analysis had to be done on unpolished crystal faces. The focused beam was necessary because of the small size of the crystals. Significant beam damage occurred during analyses. Insufficient material is available for CHN analysis, so $(NH_4)_2O$, C_2O_3, CO_2 and H_2O are calculated based on the structure (O = 13 and P = 2 *apfu* for ferriphoxite; O = 15 and P = 2 *apfu* for carboferriphoxite). The loss of volatile constituents resulted in much higher concentrations for the remaining constituents than are to be expected; therefore, the other analyzed constituents have been normalized to provide a total of 100% when combined with the calculated constituents. Analytical data are given in Table 1.

The empirical formulas for ferriphoxite (for O = 13 *apfu*) and carboferriphoxite (for O = 15 *apfu*) are $\{[(NH_4)_{2.13}K_{0.87}]_{\Sigma 3.00}(H_2O)\}\{(Fe^{3+}_{0.95}Al_{0.05})_{\Sigma 1.00}(HPO_4)_2(C_2O_4)\}$ and $\{[(NH_4)_{1.12}K_{0.88}]_{\Sigma 2.00}(H_2CO_3)\}\{(Fe^{3+}_{0.78}Al_{0.22})_{\Sigma 1.00}(HPO_4)(H_2PO_4)(C_2O_4)\}$, respectively. The ideal formula for ferriphoxite is $[(NH_4)_2K(H_2O)][Fe^{3+}(HPO_4)_2(C_2O_4)]$, which requires $(NH_4)_2O$ 12.14, K_2O 10.98, Fe_2O_3 18.61, P_2O_5 33.09, C_2O_3 16.79, H_2O 8.40, total 100 wt%. The ideal formula for carboferriphoxite is $[(NH_4)K(H_2CO_3)][Fe^{3+}(HPO_4)(H_2PO_4)(C_2O_4)]$, which requires $(NH_4)_2O$ 5.71, K_2O 10.33, Fe2O3 17.51, P_2O_5 31.13, C_2O_3 15.79, CO_2 9.65, H_2O 9.88, total 100 wt%.

X-ray crystallography

Powder X-ray studies were done using a Rigaku R-Axis Rapid II curved imaging plate microdiffractometer with monochromatized Mo*K*α radiation. A Gandolfi-like motion on the φ and ω axes was used to randomize the sample. Observed *d*-values and intensities were derived by profile fitting using JADE Pro software (Materials Data, Inc.). The powder data for ferriphoxite and carboferriphoxite are presented in Supplementary Tables 1 and 2,

https://doi.org/10.1180/mgm.2024.56 Published online by Cambridge University Press

respectively. Unit-cell parameters refined from the powder data using JADE Pro with whole pattern fitting are a = 11.357(17), b = 6. 363(17), c = 18. 818(17), β = 103.60(5)°, V = 1322(4) Å^3 and Z = 4 for ferriphoxite (space group $P2_1/c$) and a = 6.422(3), b = 9.394(3), c = 11.889(3) Å, α = 95.950(17), β = 91.852(15), γ = 100.525(17)°, V = 700.4(4) Å^3 and Z = 2 for carboferriphoxite (space group P-1).

Single-crystal X-ray studies were done using a Bruker D8 three-circle diffractometer equipped with a rotating anode generator, monochromatized Mo$K\alpha$ radiation, multilayer optics and an APEX-II CCD area detector. Empirical absorption corrections (SADABS) were applied and equivalent reflections were merged. The structures were solved using SHELXT (Sheldrick, 2015a). Refinement proceeded by full-matrix least-squares on F^2 using SHELXL-2016 (Sheldrick, 2015b).

For ferriphoxite, 11507 reflections were integrated using 38s frames with a 0.2° frame width. Systematically absent reflections are consistent with the space group $P2_1/c$. All atoms were refined with anisotropic displacement parameters. H atom sites could not be reliably extracted from the difference-Fourier map. The three large cation sites were modelled with coupled K and N (NH_4) scattering factors. One was found to be dominated by K and the other two by N. The Fe site exhibited less scattering than expected for Fe alone, so it was modelled with coupled Fe and Al. One O site corresponding to an H_2O group was found to be split into two sites 1.20 Å apart; the joint occupancies were refined to total one O *apfu*. Two P, two C and the remaining 12 O sites refined well at full occupancies.

For carboferriphoxite, 8178 reflections were integrated using 32s frames with a 0.2° frame width. The crystal had a small satellite domain rotated ~4.5° from primary domain, which led to spot splitting and additional resolved shadow spots. The best refinement was obtained by ignoring the satellite reflections. The two large cation sites were modelled with coupled K and N (NH_4) scattering factors. One is dominated by K and the other by N. The Fe site exhibited less scattering than expected for Fe alone, so it was modelled with coupled Fe and Al. Two P, three C and 15 O sites refined well at full occupancies. All H atom sites were extracted from the difference-Fourier map. The OH H sites were refined with O–H distances restrained to 0.82(2) Å and with $U_{\text{iso}}\text{H} = 1.5U_{\text{eq}}(\text{OH})$. The NH_4 H sites were refined with O–H distances restrained to 0.90(2) Å, with $U_{\text{iso}}\text{H} = 1.2U_{\text{eq}}(\text{N})$ and with H occupancies equal to the corresponding N occupancy.

Data collection and refinement details are given in Table 2. Atom coordinates, displacement parameters and site occupancies for ferriphoxite and carboferriphoxite are given in Tables 3 and 4, respectively, selected bond distances and angles for ferriphoxite and carboferriphoxite are given in Tables 5 and 6, respectively, and bond-valence analyses in Tables 7 and 9, respectively.

Descriptions of the structures

The structural units in the structures of both ferriphoxite and carboferriphoxite are topologically identical double-strand chains of corner-sharing $Fe^{3+}O_6$ octahedra and $P1O_3OH$ tetrahedra that are decorated by $P2O_3OH$ tetrahedra and C_2O_4 groups in ferriphoxite and by $P2O_2(OH)_2$ tetrahedra and C_2O_4 groups in carboferriphoxite (Fig. 4). The chain in ferriphoxite with the formula $[Fe^{3+}(C_2O_4)(PO_3OH)_2]^{3-}$ and that in carboferriphoxite with the formula $[Fe^{3+}(C_2O_4)(HPO_4)(H_2PO_4)]^{2-}$ are also topologically identical to the $[Al(C_2O_4)(PO_3OH)_2]^{3-}$ chains in thebaite-(NH_4) and dendoraite-(NH_4), which occur in the same mineral assemblage at the Rowley mine.

The interstitial complex in the ferriphoxite structure includes three large monovalent cation sites: the nine-coordinated *A*1 site ($K_{0.686}N_{0.314}$), the eight-coordinated *A*2 site ($N_{0.901}K_{0.099}$) and the ten-coordinated *A*3 site ($N_{0.772}K_{0.228}$). Bonds between O atoms in the structural units and K^+ and NH_4^+ cations at the *A*1, *A*2 and *A*3 sites link the structure in three

https://doi.org/10.1180/mgm.2024.56 Published online by Cambridge University Press

dimensions. A disordered H_2O group (W13A and W13B) in the interstitial complex is coordinated to cations at the A1 and A2 sites. The interstitial complex in the carboferriphoxite structure includes two large ten-coordinated monovalent cation sites: *A*1 ($K_{0.783}N_{0.217}$) and *A*2 site ($N_{0.871}K_{0.129}$). Bonds between O atoms in the structural units and K^+ and NH_4^+ cations in the *A*1 and *A*2 sites link the structure in three dimensions. A H_2CO_3 group in the interstitial complex is coordinated to cations at the *A*2 site and forms hydrogen bonds to the C_2O_4 group. Both structures are shown in Figure 5.

Acknowledgements

Two anonymous reviewers are thanked for constructive comments, which improved the manuscript. Mark Cooper is thanked for collecting the structure data. Ed Davis, current contractor of the Rowley mine, is thanked for allowing underground access for the study of the occurrence and the collecting of specimens. This study was funded by the John Jago Trelawney Endowment to the Mineral Sciences Department of the Natural History Museum of Los Angeles County and by a Canada Foundation for Innovation grant to FCH which funded the rotating-anode diffractometer.

References

Ferraris G. and Ivaldi G. (1988) Bond valence vs. bond length in O…O hydrogen bonds. *Acta Crystallographica*, **B44**, 341–344.

Frost, R.L. and Hales, M.C. and Wain, D.L. (2008a) Raman spectroscopy of smithsonite. *Journal of Raman Spectroscopy*, **39**, 108-114.

Frost, R.L., Locke, A. and Martens, W.N. (2008b) Synthesis and Raman spectroscopic characterisation of the oxalate mineral wheatleyite $Na_2Cu^{2+}(C_2O_4)_2 \cdot 2H_2O$. *Journal of Raman Spectroscopy*, **39**, 901–908.

https://doi.org/10.1180/mgm.2024.56 Published online by Cambridge University Press

Frost, R.L., Palmer, S.J. and Pogson, R.E. (2011) Raman spectroscopy of newberyite Mg $(PO_3OH){\cdot}3H_2O$: A cave mineral. *Spectrochimica Acta Part A: Molecular and Biomolecular Spectroscopy*, **79**, 1149–1153.

Gagné, O.C. and Hawthorne, F.C (2015) Comprehensive derivation of bond-valence parameters for ion pairs involving oxygen. *Acta Crystallographica*, **B71**, 562–578.

García-Rodríguez, L., Rute-Pérez, Á., Piñero, J.R. and González-Silgo, C. (2000) Bond-valence parameters for ammonium-anion interactions. *Acta Crystallographica*, **B56**, 565–569.

Kampf, A.R., Cooper, M.A., Nash, B.P., Cerling, T., Marty, J., Hummer, D.R., Celestian, A.J., Rose, T.P. and Trebisky, T.J. (2017) Rowleyite, $[Na(NH_4,K)_9Cl_4][V^{5+,4+}{}_2(P,As)O_8]_6{\cdot}n[H_2O,Na,NH_4,K,Cl]$, a new mineral with a mesoporous framework structure. *American Mineralogist*, **102**, 1037–1044.

Kampf, A.R., Cooper, M.A., Rossman, R.R., Nash, B.P., Hawthorne, F.C. and Marty, J. (2019a) Davidbrownite-(NH_4), $(NH_4,K)_5(V^{4+}O)_2(C_2O_4)[PO_{2.75}(OH)_{1.25}]_4{\cdot}3H_2O$, a new phosphate-oxalate mineral from the Rowley mine, Arizona, USA. *Mineralogical Magazine*, **84**, 869-877.

Kampf, A.R., Celestian, A.J., Nash, B.P. and Marty, J. (2019b) Phoxite, $(NH_4)_2Mg_2(C_2O_4)(PO_3OH)_2(H_2O)_4$, the first phosphate-oxalate mineral. *American Mineralogist*, **103**, 973–979.

Kampf, A.R., Celestian, A.J., Nash, B.P. and Marty, J. (2021a) Allantoin and natrosulfatourea, two new bat–guano minerals from the Rowley mine, Maricopa County, Arizona, U.S.A. *Canadian Mineralogist*, **59**, 603-616.

Kampf, A.R., Cooper, M.A., Celestian, A.J., Nash, B.P. and Marty, J. (2021b) Thebaite-(NH_4), $(NH_4,K)_3Al(C_2O_4)(PO_3OH)_2(H_2O)$, a new phosphate-oxalate mineral from the Rowley mine, Arizona, USA. *Mineralogical Magazine* **85**, 379-386.

https://doi.org/10.1180/mgm.2024.56 Published online by Cambridge University Press

Kampf, A.R., Cooper, M.A., Celestian, A.J., Ma, C. and Marty, J. (2022a) Dendoraite-(NH_4), a new phosphate-oxalate mineral related to thebaite-(NH_4) from the Rowley mine, Arizona, USA. *Mineralogical Magazine*, **86**, 531-538.

Kampf, A.R., Cooper, M.A., Celestian, A.J., Ma, C. and Marty, J. (2022b) Relianceite-(K), a new phosphate-oxalate mineral related to davidbrownite-(NH_4) from the Rowley mine, Arizona, USA. *Mineralogical Magazine*, **86**, 539-547.

Sergeeva, A.V., Zhitova, E.S and Bocharov, V.N. (2019) Infrared and Raman spectroscopy of tschermigite, $(NH_4)Al(SO_4)_2 \cdot 12H_2O$. *Vibrational Spectroscopy*, **105**, 102983.

Sheldrick, G.M. (2015a) SHELXT – Integrated space-group and crystal-structure determination. *Acta Crystallographica*, **A71**, 3–8.

Sheldrick, G.M. (2015b) Crystal structure refinement with SHELX. *Acta Crystallographica*, **C71**, 3–8.

Števko, M., Sejkora, J., Uher, P., Cámara, F., Škoda, R. and Vaculovič, T. (2018) Fluorarrojadite-(BaNa), $BaNa_4CaFe_{13}Al(PO_4)_{11}(PO_3OH)F_2$, a new member of the arrojadite group from Gemerská Poloma, Slovakia. *Mineralogical Magazine*, **82**, 863–876.

Wilson, W.E. (2020) The Rowley mine, Painted Rock Mountains, Maricopa County, Arizona. *Mineralogical Record*, **51**, 181–226.

Yakovenchuk, V.N., Pakhomovsky, Y.A., Konopleva, N.G., Panikorovskii, T.L.. Bazai, A., Mikhailova, J.A., Bocharov, V.N., Ivanyuk, G.Yu. and Krivovichev, S.V. (2018) Batagayite, $CaZn_2(Zn,Cu)_6(PO_4)_4(PO_3OH)_3 \cdot 12H_2O$, a new phosphate mineral from Këster tin deposit (Yakutia, Russia): occurrence and crystal structure. *Mineralogy and Petrology*, **112**, 591–601.

https://doi.org/10.1180/mgm.2024.56 Published online by Cambridge University Press

FIGURE CAPTIONS

Figure 1. Sprays of ferriphoxite blades with quartz on hematite and baryte on holotype specimen #76303; FOV 0.56 mm across.

https://doi.org/10.1180/mgm.2024.56 Published online by Cambridge University Press

Figure 2. Sprays of carboferriphoxite needles on holotype specimen #76304; FOV 0.68 mm across.

https://doi.org/10.1180/mgm.2024.56 Published online by Cambridge University Press

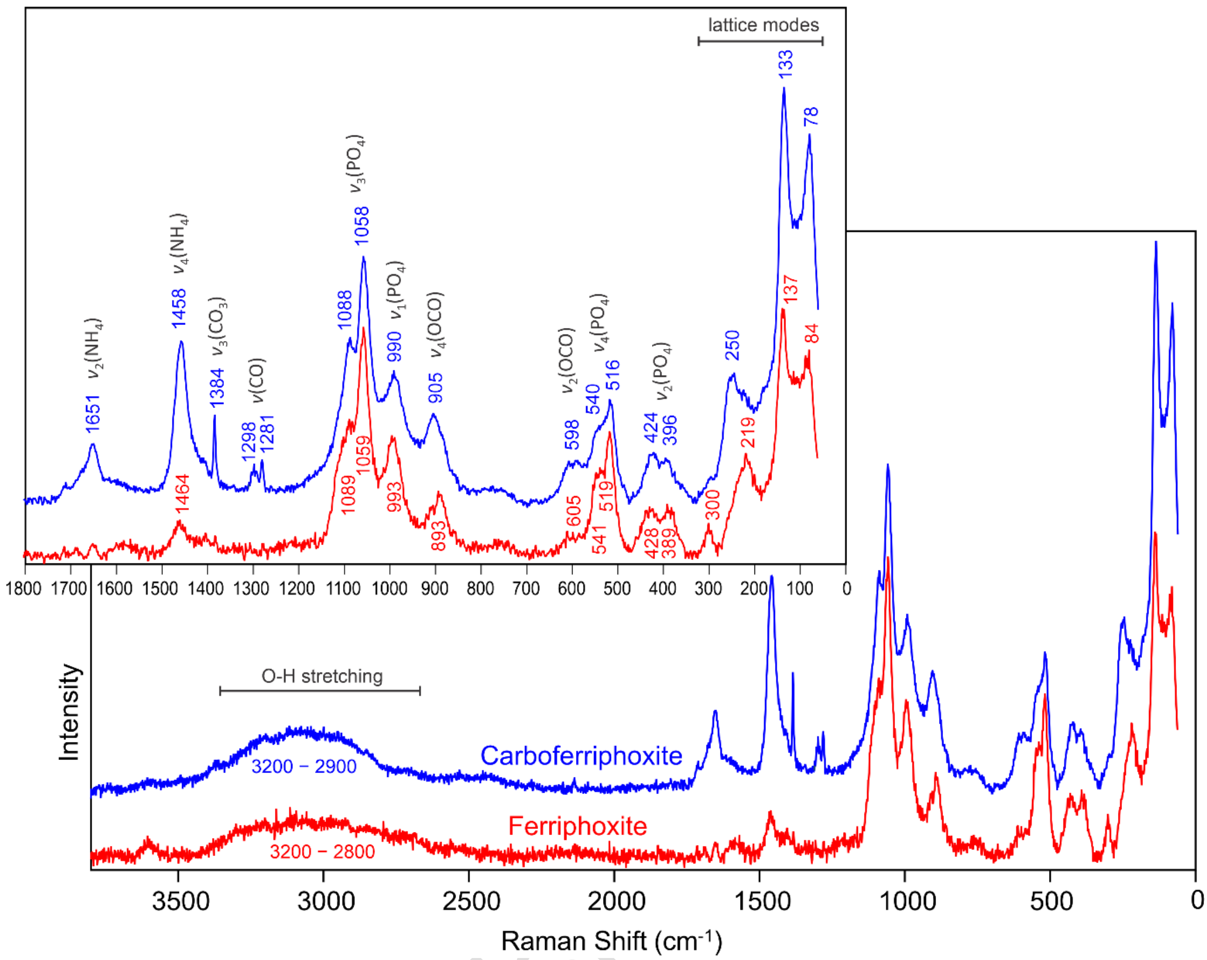

Figure 3. Raman spectra of ferriphoxite and carboferriphoxite.

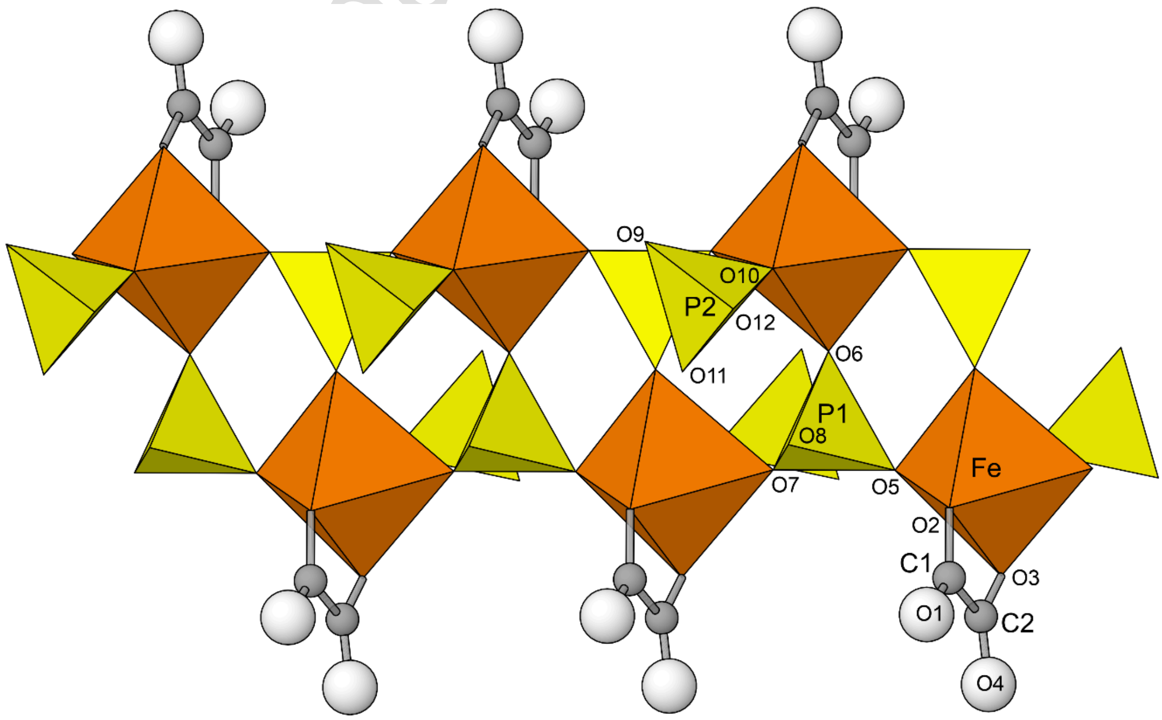

https://doi.org/10.1180/mgm.2024.56 Published online by Cambridge University Press

Figure 4. The chain along [010] in ferriphoxite and along [100] in carboferriphoxite.

Hydrogen atoms for carboferriphoxite are not shown.

https://doi.org/10.1180/mgm.2024.56 Published online by Cambridge University Press

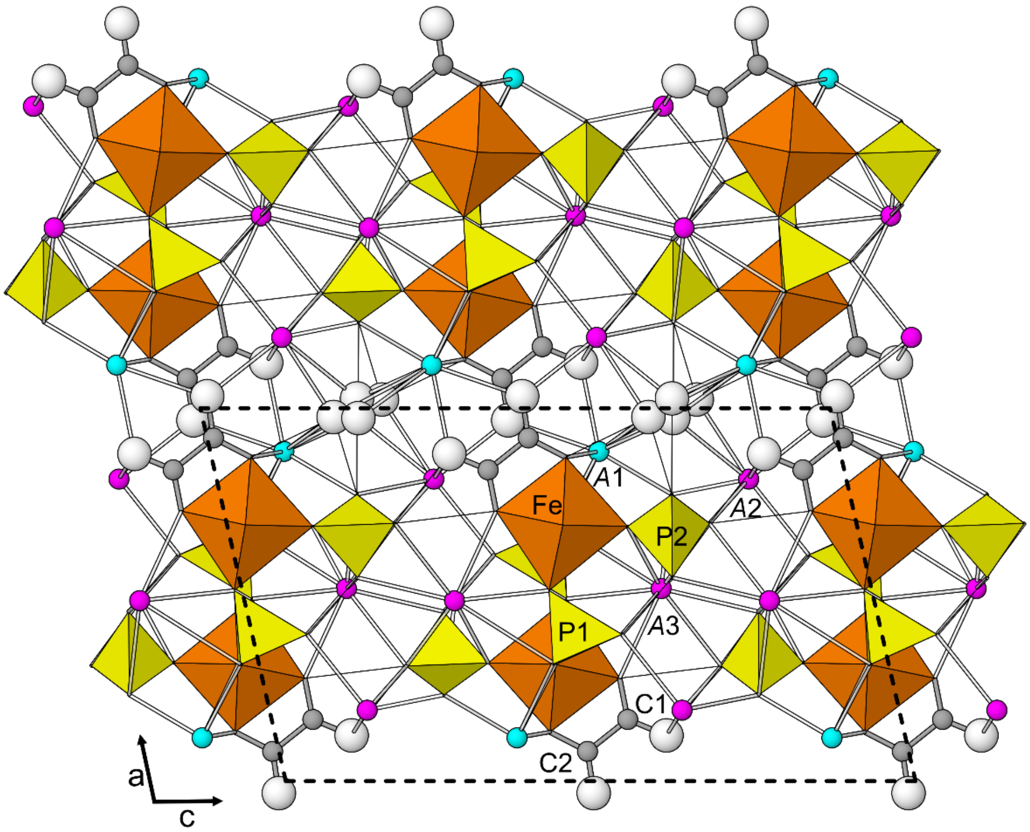

ferriphoxite

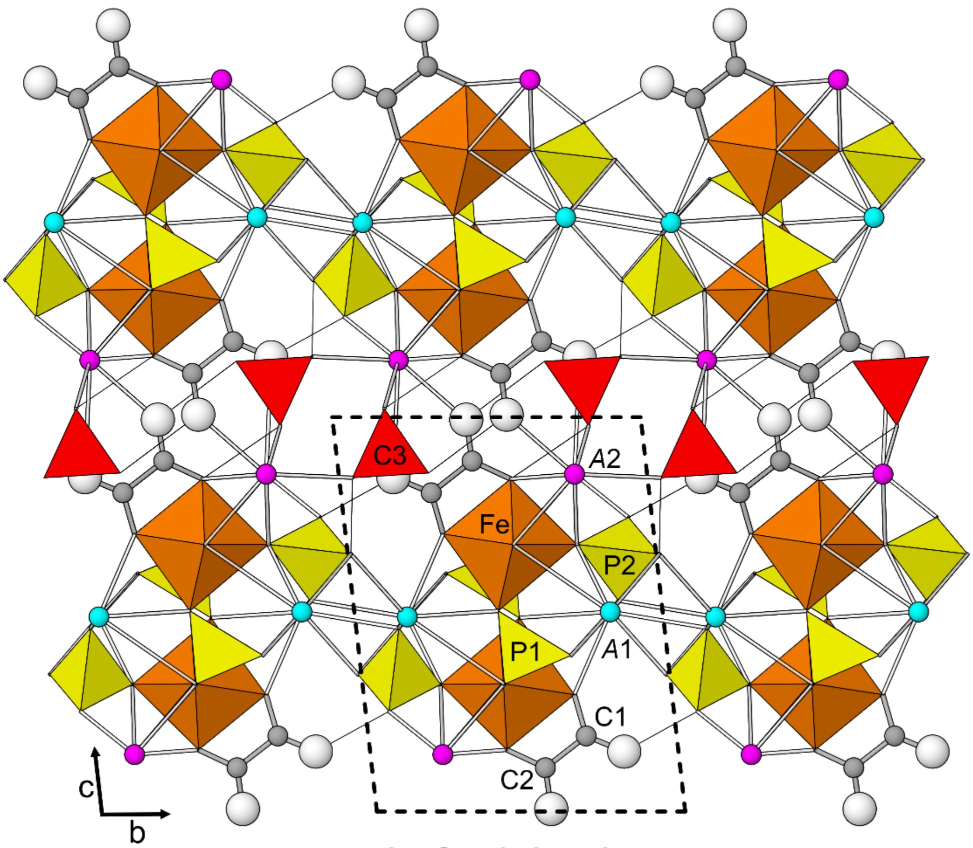

carboferriphoxite

https://doi.org/10.1180/mgm.2024.56 Published online by Cambridge University Press

Figure 5. The structures of ferriphoxite and carboferriphoxite. White balls are O atoms. The K-dominant *A* sites are turquoise and the NH_4-dominant *A* sites are pink. H atoms for carboferriphoxite are not shown. Thin black lines are hydrogen bonds. The unit cell outline is shown with dashed lines.

https://doi.org/10.1180/mgm.2024.56 Published online by Cambridge University Press

Table 1. Analytical data (wt%) for ferriphoxite and carboferriphoxite.

Const.	Ferriphoxite (4 points)				Carboferriphoxite (6 points)				Standard
	Mean	Range	S.D.	Norm.	Mean	Range	S.D.	Norm.	
$(NH_4)_2O$	11.48	10.97–12.68	0.80	*13.06	5.75	5.19–6.92	0.62	*6.51	GaN
K_2O	10.50	10.36–10.75	0.18	9.64	11.28	10.38–11.75	0.35	9.29	microcline
Al_2O_3	0.59	0.58–0.61	0.02	0.55	3.09	2.62–3.44	0.33	2.54	microcline
Fe_2O_3	19.50	19.23–19.70	0.23	17.91	16.83	16.11–17.81	0.69	13.86	fayalite
P_2O_5	36.38	36.04–36.62	0.29	33.41	38.54	37.92–39.23	0.67	31.76	apatite
C_2O_3				*16.95				*16.12	
CO_2				–				*9.84	
H_2O				*8.48				*10.08	
Total				100.00				100.00	

* Calculated based on the structures (ferriphoxite: O = 13 and P = 2; carboferriphoxite: O = 15 and P = 2).

https://doi.org/10.1180/mgm.2024.56 Published online by Cambridge University Press

Table 2. Data collection and structure refinement details for ferriphoxite and carboferriphoxite.

	Ferriphoxite		Carboferriphoxite	
Diffractometer	Bruker D8 three-circle; multilayer optics; APEX-II CCD			
X-ray radiation / source	Mo*K*α (λ = 0.71073 Å) / rotating anode			
Temperature	293(2) K			
Structural Formula (incl. unlocated H)	$\{[K_{0.676}(NH_4)_{0.324}]$ $[(NH_4)_{0.884}K_{0.116}]$ $[(NH_4)_{0.769}K_{0.231}](H_2O)\}$ $\{(Fe^{3+}{}_{0.955}Al_{0.045})(HPO_4)_2(C_2O_4)\}$		$\{[(NH_4)_{0.783}K_{0.217}]$ $[K_{0.871}(NH_4)_{0.129}](H_2CO_3)\}$ $\{(Fe^{3+}{}_{0.921}Al_{0.079})(HPO_4)$ $(H_2PO_4)(C_2O_4)\}$	
Space group	$P2_1/c$ (#14)		P-1 (#2)	
Unit cell dimensions	a = 11.389(5) Å b = 6.352(3) Å c = 18.716(9) Å	β = 102.887(9)°	a = 6.405(3) Å b = 9.399(5) Å c = 11.839(6) Å	α = 95.763(10)° β = 92.314(10)° γ = 100.665(8)°
V	1319.8 Å^3		695.6(6) Å^3	
Z	4		2	
Density (above formula)	2.154 g cm^{-3}		2.157 g cm^{-3}	
Absorption coefficient	1.731 mm^{-1}		1.597 mm^{-1}	
F(000)	866.1		454.5	
Crystal size	70 × 20 × 10 μm		85 × 20 × 5 μm	
θ range	2.55 to 27.56°		2.66 to 30.23°	
Index ranges	$-14 \le h \le 14$ $-8 \le k \le 8$ $-24 \le l \le 24$		$-9 \le h \le 9$ $-13 \le k \le 13$ $-16 \le l \le 16$	
Refls. collected / unique	11562 / 3037; R_{int} = 0.067		8178 / 4102; R_{int} = 0.0265	
Reflections with $I > 2\sigma_I$	1854		3602	
Completeness	99.9%		99.9%	
Refinement method	Full-matrix least-squares on F^2			
Parameters / restraints	204 / 0		250 / 25	
GoF	0.964		1.047	
Final R indices [$I > 2\sigma_I$]	R_1 = 0.0659, wR_2 = 0.1776		R_1 = 0.0417, wR_2 = 0.1127	
R indices (all data)	R_1 = 0.1091, wR_2 = 0.2117		R_1 = 0.0472, wR_2 = 0.1166	
Largest diff. peak / hole	+1.46 / –0.57 e/A^3		+1.87 / –0.62 e/A^3	

$R_{int} = \Sigma|F_o^2 - F_o^2(\text{mean})|/\Sigma[F_o^2]$. GoF = $S = \{\Sigma[w(F_o^2–F_c^2)^2]/(n–p)\}^{1/2}$. $R_1 = \Sigma||F_o|-|F_c||/\Sigma|F_o|$. $wR_2 = \{\Sigma[w(F_o^2–F_c^2)^2]/\Sigma[w(F_o^2)^2]\}^{1/2}$; $w = 1/[\sigma^2(F_o^2) + (aP)^2 + bP]$ where P is $[2F_c^2 + \text{Max}(F_o^2,0)]/3$; for ferriphoxite a is 0.1391 and b is 1.4053 and for carboferriphoxite a is 0.0623 and b is 0.7335

https://doi.org/10.1180/mgm.2024.56 Published online by Cambridge University Press

Table 3. Atom positions, displacement parameters and site occupancies for ferriphoxite.

	x/*a*	*y*/*b*	*z*/*c*	U_{eq}	Site occupancy
*A*1	0.11602(18)	0.2471(4)	0.38292(13)	0.0597(10)	$K_{0.686(12)}N_{0.314(12)}$
*A*2	0.1896(6)	0.2246(9)	0.1549(3)	0.071(3)	$N_{0.901(14)}K_{0.099(14)}$
*A*3	0.4838(4)	0.1264(6)	0.3336(2)	0.0526(17)	$N_{0.772(11)}K_{0.228(11)}$
Fe	0.68205(7)	0.24624(11)	0.53231(4)	0.0231(3)	$Fe_{0.895(10)}Al_{0.105(10)}$
P1	0.38494(12)	0.25642(19)	0.50178(7)	0.0200(4)	1
P2	0.67593(17)	0.3620(3)	0.69965(9)	0.0385(5)	1
C1	0.8348(6)	0.2400(9)	0.4341(3)	0.0319(12)	1
C2	0.9211(6)	0.2447(9)	0.5101(3)	0.0368(14)	1
O1	0.8774(5)	0.2365(9)	0.3786(3)	0.0580(16)	1
O2	0.7238(4)	0.2457(6)	0.4321(2)	0.0350(10)	1
O3	0.8684(4)	0.2454(6)	0.5628(2)	0.0349(10)	1
O4	0.0322(4)	0.2450(8)	0.5151(3)	0.0519(14)	1
O5	0.3128(3)	0.0630(5)	0.4708(2)	0.0299(9)	1
O6	0.5106(3)	0.2515(5)	0.4875(2)	0.0269(8)	1
O7	0.3134(3)	0.4470(5)	0.4667(2)	0.0277(9)	1
OH8	0.3935(4)	0.2582(6)	0.5869(2)	0.0352(10)	1
O9	0.7687(5)	0.5305(8)	0.7170(3)	0.0626(15)	1
O10	0.6828(4)	0.2228(6)	0.6357(2)	0.0382(11)	1
O11	0.5458(4)	0.4478(8)	0.6881(3)	0.0519(13)	1
OH12	0.6916(5)	0.2044(9)	0.7669(3)	0.0579(15)	1
O13A	1.0262(16)	0.024(3)	0.2521(12)	0.114(10)	0.64(3)
O13B	0.9761(18)	0.353(6)	0.7092(13)	0.093(9)	0.36(3)

	U^{11}	U^{22}	U^{33}	U^{23}	U^{13}	U^{12}
*A*1	0.0298(11)	0.093(2)	0.0527(14)	0.0207(12)	0.0021(9)	-0.0091(11)
*A*2	0.082(5)	0.062(4)	0.069(5)	-0.016(3)	0.019(3)	-0.013(3)
*A*3	0.075(3)	0.036(2)	0.050(3)	0.0024(16)	0.021(2)	0.0031(18)
Fe	0.0253(5)	0.0119(4)	0.0333(5)	-0.0014(3)	0.0090(3)	0.0000(3)
P1	0.0222(6)	0.0091(6)	0.0291(7)	-0.0011(5)	0.0064(5)	-0.0004(5)
P2	0.0554(11)	0.0288(8)	0.0302(8)	-0.0025(7)	0.0074(7)	-0.0063(8)
C1	0.035(3)	0.027(3)	0.034(3)	0.001(2)	0.009(2)	0.003(3)
C2	0.048(4)	0.025(3)	0.035(3)	-0.001(3)	0.006(3)	0.006(3)
O1	0.040(3)	0.100(5)	0.038(3)	-0.001(3)	0.017(2)	0.002(3)
O2	0.032(2)	0.035(2)	0.037(2)	-0.0017(18)	0.0072(18)	-0.0010(19)
O3	0.038(2)	0.031(2)	0.035(2)	-0.0013(18)	0.0080(18)	-0.0030(19)
O4	0.037(3)	0.073(4)	0.047(3)	0.005(2)	0.011(2)	0.001(2)
O5	0.029(2)	0.0069(16)	0.051(2)	-0.0021(15)	0.0031(18)	-0.0020(14)
O6	0.0237(18)	0.0206(19)	0.038(2)	-0.0016(16)	0.0098(15)	-0.0004(16)
O7	0.029(2)	0.0090(16)	0.043(2)	0.0021(15)	0.0034(17)	0.0023(14)
OH8	0.039(2)	0.039(2)	0.028(2)	0.0025(17)	0.0098(17)	-0.0008(19)
O9	0.086(4)	0.045(3)	0.053(3)	-0.009(2)	0.008(3)	-0.030(3)
O10	0.054(3)	0.031(2)	0.031(2)	-0.0016(17)	0.0124(19)	-0.0048(19)
O11	0.060(3)	0.047(3)	0.050(3)	-0.004(2)	0.016(2)	0.006(2)
OH12	0.075(4)	0.059(3)	0.033(3)	0.013(2)	-0.002(2)	-0.017(3)
O13A	0.105(12)	0.094(13)	0.159(19)	-0.050(13)	0.066(13)	-0.026(10)
O13B	0.055(12)	0.14(2)	0.084(15)	-0.031(16)	0.015(10)	-0.032(13)

https://doi.org/10.1180/mgm.2024.56 Published online by Cambridge University Press

Table 4. Atom positions, displacement parameters and site occupancies for carboferriphoxite.

	x/a	y/b	z/c	U_{eq}	Site occupancy
*A*1	0.78217(11)	0.17041(8)	0.49301(7)	0.0325(3)	$K_{0.783(5)}N_{0.217(5)}$
H1A	0.765(17)	0.103(9)	0.433(6)	0.039	0.217(5)
H1B	0.670(11)	0.158(12)	0.534(8)	0.039	0.217(5)
H1C	0.800(17)	0.258(6)	0.468(9)	0.039	0.217(5)
H1D	0.899(10)	0.165(12)	0.535(8)	0.039	0.217(5)
*A*2	0.2627(4)	0.7667(2)	0.85602(18)	0.0444(9)	$N_{0.871(6)}K_{0.129(6)}$
H2A	0.207(6)	0.846(3)	0.862(3)	0.053	0.871(6)
H2B	0.274(6)	0.737(4)	0.9252(19)	0.053	0.871(6)
H2C	0.399(3)	0.794(4)	0.835(3)	0.053	0.871(6)
H2D	0.195(5)	0.697(3)	0.807(3)	0.053	0.871(6)
Fe	0.23095(5)	0.46595(4)	0.33013(3)	0.01960(12)	$Fe_{0.921(5)}Al_{0.079(5)}$
P1	0.25391(9)	0.48587(6)	0.61155(5)	0.01760(14)	1
P2	0.24280(10)	0.12161(7)	0.35040(5)	0.02339(15)	1
C1	0.2925(4)	0.7043(3)	0.1929(2)	0.0283(5)	1
C2	0.2543(5)	0.5621(3)	0.1090(2)	0.0306(5)	1
C3	0.1828(5)	0.1661(3)	0.9084(2)	0.0319(5)	1
O1	0.3233(4)	0.8226(2)	0.1520(2)	0.0405(5)	1
O2	0.2881(3)	0.6844(2)	0.29625(17)	0.0315(4)	1
O3	0.2131(3)	0.4464(2)	0.15671(16)	0.0296(4)	1
O4	0.2677(5)	0.5683(3)	0.00692(19)	0.0497(6)	1
O5	0.0833(3)	0.5413(2)	0.67864(15)	0.0272(4)	1
O6	0.2567(3)	0.5321(2)	0.49227(15)	0.0268(4)	1
O7	0.4659(3)	0.5423(2)	0.67723(16)	0.0278(4)	1
OH8	0.1952(3)	0.31603(19)	0.60571(17)	0.0285(4)	1
H8	0.262(6)	0.270(4)	0.568(3)	0.043	1
OH9	0.3898(4)	0.0771(3)	0.2575(2)	0.0499(6)	1
H9	0.343(8)	-0.004(3)	0.219(4)	0.075	1
O10	0.1525(3)	0.2512(2)	0.32218(19)	0.0350(5)	1
O11	0.3503(3)	0.1402(2)	0.46672(18)	0.0330(4)	1
OH12	0.0503(3)	0.9905(2)	0.34773(17)	0.0339(4)	1
H12	-0.013(6)	0.979(5)	0.285(2)	0.051	1
O13	0.1390(4)	0.0444(2)	0.84925(19)	0.0410(5)	1
OH14	0.2060(5)	0.2899(3)	0.8607(2)	0.0523(6)	1
H14	0.228(9)	0.372(4)	0.904(4)	0.078	1
OH15	0.2087(6)	0.1726(3)	0.0216(2)	0.0600(8)	1
H15	0.243(9)	0.254(4)	0.065(4)	0.090	1

	U^{11}	U^{22}	U^{33}	U^{23}	U^{13}	U^{12}
*A*1	0.0313(4)	0.0291(4)	0.0378(4)	0.0049(3)	0.0012(3)	0.0069(3)
*A*2	0.0571(15)	0.0362(12)	0.0375(12)	0.0085(8)	0.0008(9)	0.0004(9)
Fe	0.01838(18)	0.01965(18)	0.01904(19)	-0.00053(12)	-0.00051(12)	0.00089(11)
P1	0.0172(3)	0.0186(3)	0.0162(3)	0.00115(19)	-0.00026(18)	0.00183(18)
P2	0.0261(3)	0.0189(3)	0.0249(3)	0.0022(2)	0.0029(2)	0.0032(2)
C1	0.0281(12)	0.0279(12)	0.0288(12)	0.0021(9)	0.0046(9)	0.0050(9)
C2	0.0353(13)	0.0285(12)	0.0267(12)	0.0009(10)	0.0005(10)	0.0043(10)
C3	0.0367(14)	0.0290(12)	0.0273(13)	0.0004(10)	-0.0032(10)	0.0015(10)
O1	0.0535(13)	0.0272(10)	0.0407(12)	0.0032(8)	0.0116(10)	0.0060(9)
O2	0.0366(10)	0.0307(9)	0.0253(9)	-0.0011(7)	0.0027(7)	0.0035(8)

https://doi.org/10.1180/mgm.2024.56 Published online by Cambridge University Press

O3	0.0378(10)	0.0266(9)	0.0227(9)	0.0002(7)	0.0005(7)	0.0028(7)
O4	0.088(2)	0.0365(12)	0.0226(10)	0.0037(8)	0.0058(11)	0.0072(12)
O5	0.0227(8)	0.0337(9)	0.0242(9)	-0.0040(7)	0.0004(6)	0.0072(7)
O6	0.0322(9)	0.0290(9)	0.0185(8)	0.0044(6)	-0.0003(6)	0.0033(7)
O7	0.0196(8)	0.0365(10)	0.0244(9)	-0.0029(7)	-0.0040(6)	0.0022(7)
OH8	0.0370(10)	0.0185(8)	0.0291(9)	0.0021(7)	0.0059(7)	0.0024(7)
OH9	0.0611(15)	0.0314(11)	0.0541(15)	-0.0035(10)	0.0312(12)	-0.0006(10)
O10	0.0367(10)	0.0214(9)	0.0455(12)	0.0074(8)	-0.0087(9)	0.0027(7)
O11	0.0342(10)	0.0295(9)	0.0338(10)	0.0004(8)	-0.0081(8)	0.0058(7)
OH12	0.0422(11)	0.0258(9)	0.0288(10)	0.0049(7)	-0.0027(8)	-0.0060(8)
O13	0.0594(14)	0.0278(10)	0.0317(11)	-0.0017(8)	-0.0105(10)	0.0032(9)
OH14	0.0705(17)	0.0382(13)	0.0451(14)	0.0037(10)	0.0007(12)	0.0037(12)
OH15	0.090(2)	0.0489(15)	0.0350(13)	0.0012(11)	-0.0015(13)	0.0002(14)

Table 5. Selected bond lengths (Å) for ferriphoxite.

*A*1–O1	2.702(6)	*A*3–O11	2.744(6)	P1–O5	1.519(4)
*A*1–O5	2.729(4)	*A*3–O6	2.939(6)	P1–O6	1.513(4)
*A*1–O7	2.748(4)	*A*3–O11	2.998(6)	P1–O7	1.523(4)
*A*1–W13A	2.817(17)	*A*3–OH8	3.035(6)	P1–OH8	1.574(4)
*A*1–O4	2.844(6)	*A*3–O2	3.033(6)	<P1–O>	1.532
*A*1–O9	2.883(6)	*A*3–O10	3.056(6)		
*A*1–W13B	3.12(3)	*A*3–OH12	3.103(8)	P2–O9	1.488(5)
*A*1–W13A	3.205(16)	*A*3–OH12	3.204(7)	P2–O10	1.504(4)
*A*1–O3	3.282(5)	*A*3–O9	3.564(7)	P2–O11	1.548(5)
*A*1–O13B	3.35(2)	*A*3–O5	3.576(6)	P2–OH12	1.587(5)
*A*1–O3	3.373(5)	<*A*3–O>	3.125	<P2–O>	1.532
<*A*1–O>	3.005				
		Fe–O10	1.939(4)	*Oxalate group*	
*A*2–O9	2.807(8)	Fe–O6	1.946(4)	C1–C2	1.539(9)
*A*2–O4	2.829(8)	Fe–O7	1.949(4)	C1–O1	1.240(8)
*A*2–W13B	2.88(2)	Fe–O5	1.966(4)	C1–O2	1.256(7)
*A*2–OH8	2.889(8)	Fe–O2	2.035(4)	C2–O3	1.262(8)
*A*2–W13A	3.148(17)	Fe–O3	2.072(5)	C2–O4	1.248(8)
*A*2–O1	3.221(8)	<Fe–O>	1.994		
*A*2–OH12	3.243(9)			*Hydrogen bonds*	
*A*2–O1	3.366(8)			OH8···O11	2.566(7)
*A*2–O2	3.687(7)			OH12···O1	2.649(7)
<*A*2–O>	3.048			W13A···O9	2.880(18)
				W13B···O9	2.65(2)
				W13A···W13B	2.50(3)

https://doi.org/10.1180/mgm.2024.56 Published online by Cambridge University Press

Table 6. Selected bond lengths (Å) and angles (°) for carboferriphoxite.

*A*1–O11	2.730(3)	*A*2–O4	2.713(3)	Fe–O6	1.948(2)
*A*1–O2	2.815(2)	*A*2–O5	2.869(3)	Fe–O7	1.962(2)
*A*1–OH12	2.829(2)	*A*2–O13	2.872(3)	Fe–O10	1.980(2)
*A*1–O6	2.841(2)	*A*2–OH9	2.889(3)	Fe–O5	1.999(2)
*A*1–OH8	2.943(2)	*A*2–O10	3.296(3)	Fe–O3	2.040(2)
*A*1–O11	2.978(3)	*A*2–O3	3.311(3)	Fe–O2	2.100(2)
*A*1–OH12	3.081(3)	*A*2–O7	3.311(3)	<Fe–O>	2.016
*A*1–O10	3.213(3)	*A*2–O1	3.485(4)		
*A*1–O5	3.549(2)	*A*2–OH15	3.516(5)	P1–O5	1.5145(19)
*A*1–OH9	3.604(3)	*A*2–OH15	3.551(4)	P1–O7	1.5152(18)
<*A*1–O>	3.060	<*A*2–O>	3.181	P1–O6	1.5186(19)
				P1–OH8	1.565(2)
Oxalate group		*Dihydrogen carbonate group*		<P1–O>	1.528
C1–C2	1.558(4)	C3–O13	1.258(3)		
C1–O1	1.243(3)	C3–OH14	1.331(4)	P2–O11	1.494(2)
C1–O2	1.257(3)	C3–OH15	1.337(4)	P2–O10	1.502(2)
C2–O4	1.221(4)	<C3–O>	1.309	P2–OH9	1.552(2)
C2–O3	1.265(3)			P2–OH12	1.571(2)
				<P2–O>	1.530

Hydrogen bonds (*D* = donor, *A* = acceptor)

D–H···*A*	*D*–H	H···*A*	*D*···*A*	<*DHA*
N1–H1A···OH12	0.89(2)	2.48(9)	3.081(3)	126(9)
N1–H1B···O11	0.88(2)	2.14(9)	2.730(3)	124(9)
N1–H1C···O6	0.89(2)	2.08(7)	2.841(2)	143(10)
N1–H1D···OH12	0.89(2)	2.17(9)	2.829(2)	130(9)
N2–H2A···O13	0.88(2)	2.008(19)	2.872(3)	165(4)
N2–H2B···O4	0.90(2)	1.93(3)	2.713(3)	144(3)
N2–H2C···OH9	0.91(2)	2.07(2)	2.889(3)	149(3)
N2–H2D···O5	0.87(2)	2.011(17)	2.869(3)	170(4)
OH8–H8···O11	0.79(2)	1.80(2)	2.573(3)	166(4)
OH9–H9···O1	0.84(2)	1.72(3)	2.538(3)	162(5)
OH12–H12···O13	0.82(2)	1.732(19)	2.547(3)	178(5)
OH14–H14···O4	0.87(2)	2.07(2)	2.941(4)	177(5)
OH15–H15···O3	0.86(2)	2.06(3)	2.885(4)	160(6)

https://doi.org/10.1180/mgm.2024.56 Published online by Cambridge University Press

Table 7. Bond valences analysis for ferriphoxite. Values are in valence units (*vu*).

	*A*1	*A*2	*A*3	Fe	P1	P2	C1	C2	Hydrogen bonds		Σ
									accepted	donated	
O1	0.22	0.07 0.04					1.49		0.25		2.07
O2			0.11	0.47			1.43				2.01
O3	0.05 0.04			0.42				1.41			1.92
O4	0.15	0.19						1.46			1.80
O5	0.20		0.02	0.57	1.30						2.09
O6			0.14	0.60	1.32						2.06
O7	0.19			0.59	1.29						2.07
OH8		0.16	0.11		1.13					-0.31	1.09
O9	0.14	0.20	0.03			1.41			0.25		2.03
O10			0.10	0.61		1.35					2.06
O11			0.12			1.21			0.31		1.64
OH12		0.06	0.09 0.07			1.10				-0.25	1.07
W13a	0.16 0.06	0.08							0.18	-0.38	0.10
W13b	0.07 0.04	0.17							0.26	-0.31	0.23
Σ	1.32	0.97	0.79	3.26	5.04	5.07	2.92	2.87			

Bond-valence parameters for NH_4^+–O are from Garcia-Rodriguez *et al.* (2000); all others are from Gagné and Hawthorne (2015). Hydrogen-bond valences are based on O–O bond lengths from Ferraris and Ivaldi (1988). Negative values indicate donated hydrogen-bond valence. Bond-valence values are based on refined occupancies.

https://doi.org/10.1180/mgm.2024.56 Published online by Cambridge University Press

Table 8. Bond valences analysis for carboferriphoxite. Values are in valence units (*vu*).

	*A*1	*A*2	Fe	P1	P2	C1	C2	C3	Hydrogen bonds		Σ
									accepted	donated	
O1		0.03				1.47			0.34		1.84
O2	0.16		0.39			1.42					1.97
O3		0.05	0.46				1.40		0.16		2.07
O4		0.26					1.56		0.14		1.96
O5	0.02	0.17	0.51	1.32							2.02
O6	0.15		0.59	1.30							2.04
O7		0.05	0.57	1.31							1.93
OH8	0.11			1.16						-0.31	0.96
OH9	0.02	0.16			1.20					-0.34	1.04
O10	0.06	0.05	0.54		1.36						2.01
O11	0.20 0.10				1.39				0.31		2.00
OH12	0.15 0.08				1.14					-0.33	1.04
O13		0.17						1.42	0.33		1.92
OH14								1.18		-0.14	1.04
OH15		0.03 0.03						1.17		-0.16	1.07
Σ	1.04	1.00	3.10	5.00	4.90	2.85	2.81	3.59			

NH_4^+ is treated as a spherical cation and bond-valence parameters for NH_4^+–O are from Garcia-Rodriguez *et al.* (2000); all others are from Gagné and Hawthorne (2015). Hydrogen-bond valences are based on O–O bond lengths from Ferraris and Ivaldi (1988). Negative values indicate donated hydrogen-bond valence. The cation sites were modelled using refined occupancies.

https://doi.org/10.1180/mgm.2024.56 Published online by Cambridge University Press